ASTRONOMY & ASTROPHYSICS
SUPPLEMENT SERIES
Astron. Astrophys. Suppl. Ser. **105**, 247-258 (1994)

Images of 25 extragalactic radio sources observed with MERLIN at 18 cm

Chidi E. Akujor[1,2,3,⋆], E. Lüdke[2], I.W.A. Browne[2], J.P. Leahy[2], S.T. Garrington[2], N. Jackson[2,4] and P. Thomasson[2]

[1] Onsala Space Observatory, S-439 92, Onsala, Sweden
[2] University of Manchester, Nuffield Radio Astronomy Laboratories, Jodrell Bank, Cheshire SK11 9DL, U.K.
[3] School of Physical Sciences, Imo State University, Owerri, Imo State, Nigeria
[4] Leiden Observatory, Leiden, The Netherlands

Received May 25; accepted September 24, 1993

Abstract. — We present high resolution observations of 25 extragalactic radio sources made with MERLIN at 1.6 GHz. These objects, comprising quasars and galaxies, have been mapped with angular resolutions from 0.15 to 0.35 arcsecs. The observational parameters of each source and information on previously published data are also presented

Key words: quasar — galaxy: jets — radio continuum: galaxies

1. Introduction

In recent years much has been learnt about the radio structure of extragalactic radio sources through high resolution observations made with the VLA, MERLIN and *VLBI*. MERLIN observations have been particularly useful for offering high angular resolution even at low frequencies, such that direct comparison with VLA images (of comparable resolution) at high frequencies has been possible (e.g. Leahy et al. 1989). The radio images of several powerful sources observed with MERLIN have been published (e.g. Leahy et al. 1989, Spencer et al. 1989, Akujor et al. 1991).

Here, a further 25 MERLIN images of extragalactic radio sources from the 3C and 4C catalogues observed at 1.6 GHz are presented. These observations have been made for a number of projects and for one reason or another have not previously been published. The majority of objects are high-redshift ($z \geq 1$) radio galaxies and quasars, but we also include some interesting low-z objects.

2. Observations

The observations were made at 1665 MHz and taken over the period 1980 to 1989, each observation lasting on the average 14 hours (see Table 1). The details of the MERLIN array configuration have been described by Thomasson (1986). For most of the observations we employed the six antennae of MERLIN (Lovell (or MK2), Defford, Darnhall, Wardle, Knockin and Tabley). For a few more recent observations (see Table 1) the 18 m central element of the Cambridge One-Mile telescope was added to the array, thus improving not only the angular resolution but also the East–West *uv* coverage, which is particularly useful for low declination sources.

For each observation one of the following sources was used for initial corrections of antenna gains and the correlator based closure offsets: BL Lac, 2134+004 or 0552+398; flux densities were determined with observations of 3C286 and 3C287 on the scale of Baars et al. (1977). The initial calibration was done in Jodrell Bank OLAF package written by R. Noble and others. Further processing used the self–calibration technique (Cornwell & Wilkinson 1981) in the OLAF difference-mapping program, 'MAP' and the NRAO AIPS routines. The restoring beams vary from 0.35 to 0.15 arcsec depending on whether the baselines were extended to Cambridge, and whether we needed to display extended low brightness features in the maps.

3. Results

The images (Fig. 1) and observational parameters (Table 1) are presented in order of increasing right ascension. The dynamic range (defined as peak surface brightness $S_{\rm pk}$ to rms off source, $\sigma_{\rm rms}$) varies from 100:1 to better than 1000:1 in brighter sources. In sources with significantly ex-

Send offprint requests to: Chidi E. Akujor*
⋆Present address: Max Planck Inst. für Radioastronomie, Auf dem Hügel 69, D-53121 Bonn, Germany

tended structure or strong bridge emission, the flux densities in our maps appear to be systematically lower than the total flux densities from single dish observations (Kühr et al. 1979). This is due to the extended weak features being resolved out by MERLIN due to the absence of short spacings in the array.

4. Comments on individual sources

0017+153, 3C9, *quasar* : VLA maps have been published (Lonsdale & Barthel 1987; Swarup et al. 1982; Garrington et al. 1991). Our map shows the knotty one–sided jet. The radio core detected in the Lonsdale & Barthel map (3.5 mJy) and closely coincident with the optical position is not seen in our map. We, therefore, estimate the core spectral index, α, ($S \sim \nu^{-\alpha}$) to be ≤ -0.2. This quasar is a prototype 'hotspotless' source, a class which is currently a subject of intense investigation (see Akujor & Garrington 1993). The total flux density in our map is only about 50% of the source flux density (Kühr et al. 1979). Most of the missing flux density would reside in the extended structure associated with the northern lobe and surrounding the jet as seen by Garrington et al.

0033+182, 3C14, *quasar* : Garrington et al., have published low resolution VLA maps at 6 and 18 cm. Our map shows that the weak radio core detected by Garrington et al., has a steep spectrum α=0.7. The bridge emission and the jet which connects the core to the southern hotspot as seen in Garrington et al., are not evident in our higher resolution map. This could account for about 40% of total flux density missing in our high resolution map.

0134+325, 3C48, *quasar* : Our map barely resolves the structure of the powerful compact radio source. Previous maps include the 15 GHz VLA map of van Breugel et al. (1984), the world array ($VLBI$) map of Wilkinson et al. (1991), low resolution $VLBI$ map of Simon et al. (1990) and 5 GHz MERLIN map (Akujor et al. 1991). The radio core (see Wilkinson et al. 1991) is associated with the southern tip of its structure.

0232−043, 4C−04.06, *quasar*: This source shows a triple structure as seen in earlier maps of Hintzen et al. (1981). The central component (see also Garrington et al. 1991) has a flat spectrum, $\alpha = -0.08$, and is therefore the core component. This component also has a slight extension to the west, which could be part of the bridge emission or evidence of a jet pointing to the western lobe. There is also a possible double hotspot structure in the counter–lobe.

0802+102, 3C191, *quasar* : Previously published maps of this object include the MERLIN map of Cawthorne et al. (1986) and the VLA map of Kronberg et al. (1990). Our new MERLIN map has higher resolution than Cawthorne et al., map and shows more clearly the details of the knotty southern jet.

0850+140, 3C208, *quasar* : This source has a double–lobed asymmetric structure with a weak and compact central component. Our map suggests that the structure of the eastern component is simpler than is suggested by the earlier MERLIN map of Cawthorne et al. (1986). However, a more recent MERLIN map (Roland & Akujor, private communication) shows that the hotspots in both lobes are well set back from the outermost edges, and the core and lobes are associated with surrounding radio emission. In comparison with single dish flux density, our map contains only about 50% of the source total flux density (Kühr et al. 1979). The missing flux density may reside in the surrounding emission seen in the Roland and Akujor map.

0955+324, 3C232, *quasar*: The object shows a slight extension in P.A. $\sim 50°$. It has attracted interest because there is a low luminosity galaxy NGC3067 about 2 arcmin to the South (Carilli et al. 1989). Compared with a MERLIN 408 MHz map (Akujor and Browne, private comm.), the source has a flat spectrum $\alpha \sim 0.2$ (see also Perley 1982).

1003+350, 3C236, *galaxy* : The giant double radio galaxy 3C236 has an extended core component with 1 arcsec diameter. VLA observations at 4.9, 14.8 and 22.5 GHz show an elliptical core with a 'finger' of emission pointing towards the northeast lobe (Fomalont et al. 1979). Later VLB 20 cm maps at 5 mas resolution show three aligned knots (Schilizzi et al. 1988). The MERLIN map presented here shows a resolved core rather like that in the previous VLA maps.

1038+064, 4C06.04, *quasar*: The core-jet structure seen by Akujor and McGruder (1991) can be recognized in the slight southwestern extension seen in our map. Burns et al. (1981) suggest this quasar belongs to a cluster of galaxies.

1040+123, 3C245, *quasar*: Earlier MERLIN maps at 408 and 1666 MHz of this superluminal quasar have been published (Foley & Barthel 1990). Our new map confirms the triple structure and one–sided jet in this powerful source and also shows that the North–South features in their map are artifacts possibly caused by the low declination of the source.

1056+432, 3C247, *galaxy*: Our very sensitive map shows the extended double–lobed structure as seen in VLA maps (Liu et al. 1992). However, more details of the substructure within the lobes are seen due to much higher resolution of our map. The radio core seen at 5 GHz by Liu et al., is not detected in our map, indicating a core spectral index of ≤ 0.2.

1140+222, 3C263.1, *galaxy*: Our map shows a double radio structure and a complex hotspot structure in the southwest lobe. The bright compact hotspot accounts for 10% of the total flux density at 1.6 GHz. The core seen in 5 GHz VLA maps (Liu et al. 1992; Akujor & Browne, in prep.) is not detected in our map, which imples a core spectral index of ≤ 0.3.

1218+336, 3C270.1, *quasar*: This source has been classified as a 'dog–leg' or bent quasar. Previous maps have been published (Stocke et al. 1985; Garrington et al. 1991). Our higher resolution map shows a bright core with a flux density of 121 mJy. The 5 GHz VLA map (Stocke et al. 1985) shows a prominent knot close to the Southern lobe which is likely to be part of a jet to the South. About 40% of the source flux density (Kühr et al. 1978) is missing in our map which is likely to be due to a strong bridge emission which we do not detect.

1241+164, 3C275.1, *quasar*: This is another 'dog–leg' quasar. Previously published maps include those of Stocke et al. (1985), Garrington et al. (1991) and Liu & Pooley (1990). The distortion of the nothern component is thought to be related to an interaction between the quasar and a companion galaxy close to the Northern lobe (Hintzen et al. 1981). As for 3C270.1, 40% of the flux is missing in our high-resolution map.

1253−055, 3C279, *quasar*: This is the first radio source in which superluminal motion was detected, with $v \sim 10c$ (Cohen et al. 1971). It has a double structure at low frequencies (Browne et al. 1982) and a core–jet structure at high resolution (de Pater & Perley 1983). Our map shows clearly the details of the core–jet structure as seen in the high resolution VLA maps.

1258+402, 3C280.1, *quasar*: Our map shows a bright compact lobe and a bent prominent jet which terminates without a hotspot. Previously published maps include those of Swarup et al. (1982) and Garrington et al. (1991). Our high resolution map contains about 50% of the flux density given by Kühr et al. (1979).

1328+304, 3C286, *quasar*: This source is usually classified as a compact steep–spectrum source, and previous VLA maps (Spencer et al. 1991) and a MERLIN map at 5 GHz (Akujor et al. 1991) have been published. Our high dynamic range map, however, is the most revealing yet made of this source at high resolution, and shows a knotty jet and a two–sided structure. The extension East of the core is also seen in the 408 MHz map of Saikia (1989). 3C286 has been claimed to show a two–sided structure on pc-scale (Spencer et al. 1991).

1340+603, 3C288.1, *quasar*: Our map shows a two–component structure. However, a new VLA 8.4 GHz map (Akujor & Garrington, in preparation) shows the compact component to the East to be a knotty jet surrounded by a weak diffuse emission. At 8.4 GHz a weak radio core is also detected at the position of the weak central feature marked in our map.

1409+524, 3C295, *galaxy*: This is a very luminous radio source sometimes classified as a compact steep–spectrum source. Previous maps at different frequencies have been published (Akujor et al. 1989; Perley & Taylor 1991). Our map has better sensitivity and higher resolution than the earlier 1.6 GHz MERLIN map by Akujor et al. The main features of the source–the NW lobe with multiple hotspots and the SE lobe with its extended arc and a bright hotspot are resolved.

1441+521, 3C303, *galaxy*: Our map shows a one–sided jet structure and details of the western hotspot complex but a recent lower resolution VLA map (Leahy & Perley 1991) shows that this source has faint but complex hotspot to the East and a surrounding steep–spectrum cocoon. The eastern hotspot is not detected due to low surface brightness sensitivity of our map. The VLA map also shows that the western hotspot whose details are clearly revealed in our map is well set back from the source edge.

1547+213, 3C324, *galaxy*: Our map shows the simple double structure with a more compact and brighter eastern component, consistent with the VLA images of Pedelty et al. (1987). About 40% of the source flux density measured by Kühr et al. (1979) is missing in our high resolution map.

1553+201, 3C326.1, *galaxy*: This source is one of the most distant 3CR radio galaxies at $z = 1.825$ redshift and has been suggested to be a proto–galaxy on the basis of its enormous Lyα luminosity (McCarthy et al. 1987). Our map shows a double–lobed structure consistent with published VLA image (McCarthy et al. 1987). The brighter and more compact hotspot to the West is closely coincident with the peak of bright emission–line gas.

1709+460, 3C352, *galaxy* : A previous 5 GHz VLA map by Schilizzi et al. (1982) shows a double structure. At similar resolution (1.2 arcsec) Garrington et al. (1991) detected a C-shape symmetry in the lobes. Our MERLIN map shows double hotspot structure in each lobe.

1759+135, 4C13.66, *galaxy ?*: This compact steep-spectrum source is one of the objects added to the complete "3C" sample by Laing, Riley & Longair (1983). This is now the only object in that sample lacking a redshift; recently Laing (priv. comm.) has obtained an optical spectrum at the radio position and discovered faint continuum emission ($m_V \sim 23$) but no definite emission lines. The object is thus probably a very distant galaxy. The radio structure is dominated by two resolved components separated by $1\rlap{.}''11$. The very faint emission extending several arcsec to the NW is confirmed by a 4.9 GHz VLA map (R. Laing, priv. comm). The unusual structure with faint emission extending well beyond the compact 'hotspots' is shared by some other high-redshift objects, e.g. the quasar 3C190 (Pearson et al. 1985) and the galaxy 4C41.17 (Chambers et al. 1990).

1807+697, 3C371, *galaxy/BL Lac*: Our map of this source shows a bright core and a one–sided jet extending out to $\sim$ 3 arcsec from the core. A high dynamic range VLA map (Wrobel & Lind 1990) shows faint extension of the jet out to 25 arcsec, and a faint twin–lobes straddling the core–jet structure. Wrobel & Lind interpret the structure as an edge–brightened double viewed at a large enough angle that the radio lobes only marginally overlap. The associated low brightness emission detected by Wrobel and Lind could account for about 40% of the source flux density (Kühr et al. 1978) missed in our map.

Acknowledgements. CEA acknowledges the award of Leverhulme Fellowship and is grateful to Prof R.D. Davies for encouragement. EL acknowledges the award of a PhD scholarship from the Brazilian institution CAPES.

References

Akujor C.E., Spencer R.E. & Wilkinson P.N. 1990, MNRAS 244, 362
Akujor C.E. & McGruder III C.H. 1991, In: eds. Millar H.R. & Witta P.J., Variability of Active Galactic Nuclei (Cambridge Univ. Press) p. 169
Akujor C.E. Spencer R.E., Zhang F.J., Browne I.W.A. & Fanti C. 1991, MNRAS 250, 214
Akujor C.E. & Garrington S.T. 1993, eds. R.J. Davis & R.S. Booth, Subarcsecond Radio Astronomy (Cambridge Univ. Press)
Baars J.W.M., Genzel R., Paulini-Toth I.I.K. & Witzel A. 1977, A&A 61, 99
Bridle A.H., Fomalont E.B. & Cornwell T.J. 1981, AJ 86, 1294
Browne I.W.A. et al. 1982, Nature 299, 788
Carilli C. et al. 1989, Nature 338, 134
Cawthorne T.V., Scheuer P.A.G., Morison I. & Muxlow T.W.B. 1986, MNRAS 219, 883
Chambers K.C., Miley G.K., van Breugel W.J.M. 1990, ApJ 363, 21
Cohen M. et al. 1971, ApJ 170, 207
Cornwell T.J. and Wilkinson P.N. 1981, MNRAS 196, 1067
de Pater I. & Perley R.A. 1983, ApJ 273, 64
Foley A.R. and Barthel P.D. 1990, A&A 228, 17
Fomalont E.B., Miley G.K. & Bridle A.H. 1979, A&A 76, 106
Garrington S.T., Conway R.G. and Leahy J.P. 1991, MNRAS 250, 171
Kronberg P.P., Perry, J.J. and Zukowsky E.L.H. 1990, ApJ 355, L31
Kühr H., Nauber U., Pauliny-Toth I.I.K, Witzel A. 1979, MPIfR Preprint Nr 55
Hintzen P., Boeshaar G.O. & Scott J.S. 1981, ApJ 246, L1
Leahy J.P. Muxlow T.W.B. & Stephens P.W. 1989, MNRAS 239, 401
Leahy J.P. & Perley R.A. 1991, AJ 102, 537
Laing R.A., Riley J.M. & Longair M.S. 1983, MNRAS 204, 151
Liu R. & Pooley G. 1990, MNRAS 245, p. 17
Liu R., Pooley G. & Riley J.M. 1992, MNRAS 257, 545
Lonsdale C.J. and Barthel P.D. 1987, AJ 94, 1487
McCarthy P.J. et al. 1987, ApJ 319, L39
Pearson T.J., Perley R.A. & Readhead A.C.S. 1985, AJ 90, 738
Pedelty J.A. et al. 1989, AJ 97, 647
Perley R.A. 1982, AJ 87, 859
Perley R.A. & Taylor G.B. 1991, AJ 101, 1623
Saikia D.J. 1989. In Extranuclear Activity in Galaxies, eds. E.J.A. Meurs & R.A.E. Fosbury, ESO Proc. no 32, p. 71
Schilizzi R.T., Kapahi V.K. & Neff S.G. 1982, JAA 3, 173
Schilizzi R.T. et al. 1988, eds. M.J. Reid & J.M. Moran, in The Impact of *VLBI* in Astrophys. and Geophysics, IAU Symp. 129 (D. Reidel) p. 127
Simon R.S., Readhead A.C.S., Moffet A.T., Wilkinson P.N. & Anderson B. 1980, ApJ 236, 707
Simon R.S., Readhead A.C.S., Moffet A.T., Wilkinson P.N., Booth R., Allen B. & Burke B.F. 1990, ApJ 354, 140
Spencer R.E. et al. 1989, MNRAS 240, 657
Spencer R.E. et al. 1991, MNRAS 250, 225
Stocke J.T., Burns J.O. and Cristiansen W.A. 1985, ApJ 299, 799
Swarup G. et al. 1982, MNRAS 201, 393
Thomasson P. 1986, QJRAS 27, 413
Thompson A.R. et al. 1980, ApJS 44, 151
van Breugel W., Miley G., Heckman T. 1984, AJ 89, 5
Wilkinson P.N., Spencer R.E., Readhead A.C.S, Pearson T.J. & Simon R.S. 1984, In: *VLBI* and Compact Radio Sources, IAU Symp. No. 110, eds. R. Fanti, R. Kellermann & G. Setti (D. Reidel, Dordrecht) p. 25
Wilkinson P.N., Tzioumis A.K., Akujor C.E., Benson J.M, Walker R.C. & Simon R.S. 1990, In: Parsec–scale Radio Jets, eds. J.A. Zensus & T.J. Pearson (Camb. Univ. Press, Cambridge) p. 152
Wilkinson P.N., Tzioumis A.K., Simon R.S., Benson J.M, Walker R.C 1990, Nature 352, 313
Wrobel J.M. and Lind K.R. 1990, ApJ 348, 135

Table 1. Observational parameters of the sample

IAU	3CR/4C	ID	z	LAS(″)	LLS(kpc)	Date	Beam(″)	Comp.	S(mJy)	α	S_{pk}(mJy/b)	σ_{rms}(mJy/b)
0017+153	3C9	Q	2.012	13.5	55.2	16/02/82	0.35	Total	786	1.09	145	1.0
								Jet	578			
								NW	208			
0033+182	3C14	Q	1.469	26.0	111.3	04/02/89	0.35	Total	958	0.81	147	1.0
								S	346			
								Core	21			
								N	591			
0134+325	3C48	Q	0.367	1.6	4.9	14/02/82	0.25	Total	13212	0.59	6846	2.3
0232-043	4C-04.06	Q	1.434	17.5	75.0	19/02/87	0.25	Total	692		173	1.0
								W	363			
								Core	179			
								E	150			
0802+102	3C191	Q	1.954	5.0	20.6	25/01/83	0.25	Total	1175	0.98	262	1.0
								N	498			
								Core	28			
								Jet	649			
0850+140	3C208	Q	1.110	2.4	10.3	12/11/82	0.25	Total	914	0.96	307	2.2
								W	52			
								Core	25			
								E	837			
0955+324	3C232	Q	0.533	0.6	2.2	15/05/88	0.25	Total	893	0.22	894	0.3
1003+350	3C236	G	0.099	1.2	1.5	15/05/84	0.25	Total	2778	0.51	1449	0.7
								NW	863			
								SE	1915			
1038+064	4C06.04	Q	1.270	0.8	3.5	14/05/88	0.25	Total	1292		1292	1.2
1040+123	3C245	Q	1.028	5.4	23.0	03/02/87	0.22	Total	2334	0.78	1601	0.4
								Core	1635			
								Jet	699			
1056+432	3C247	G	0.749	7.0	28.7	25/01/83	0.25	Total	2660	0.61	503	1.2
								NE	952			
								SW	1709			
1140+222	3C263.1	G	0.824	5.0	20.7	22/12/88	0.20	Total	2046	0.87	438	0.7
								NE	1138			
								Stotal	908			
								SWlobe	516			
1218+336	3C270.1	Q	1.520	10.8	46.1	16/05/84	0.35	Total	1345	0.75	309	0.8
								N	225			
								Core	121			
								Jet	969			
1241+164	3C275.1	Q	0.557	18.2	67.5	05/02/89	0.35	Total	1595	0.96	195	1.2
								S	931			
								Core	181			
								N	483			
1253-055	3C279	Q	0.538	15.0	54.9	20/02/83	0.35	Total	9089	0.02	7989	1.4
								Core	7998			
								Jet	1093			
1258+402	3C280.1	Q	1.659	4.7	19.9	09/11/82	0.25	Total	523	0.93	103	1.1
								W	360			
								Jet	168			
1328+304	3C286	Q	0.849	6.1	25.4	15/11/86	0.25	Total	13688	0.24	6807	1.0
								Core	13000			
								W Jet	416			
								E Jet	271			
1340+603	3C288.1	Q	0.961	8.5	36.0	22/11/82	0.25	Total	1074	0.84	326	0.5
								E	294			
								W	779			
1409+524	3C295	G	0.461	4.7	16.1	15/03/89	0.15	Total	19454	0.63	2906	1.6
								NW	9312			
								SE	10142			
1441+521	3C303	G	0.141	47.0	76.4	14/11/82	0.35	Total	1669	0.76	1037	0.5
								Core	1037			
								Jet	14			
								Lobe	618			
1547+213	3C324	G	1.207	17.3	74.5	30/04/84	0.25	Total	1226	0.86	258	0.7
								SW	304			
								NE	922			
1553+201	3C326.1	G	1.820	7.6	31.7	18/01/87	0.25	Total	1781	0.15	1029	0.3
								E	375			
								W	1406			
1709+460	3C352	G	0.806	13.5	55.6	05/02/89	0.35	Total	1361	0.88	181	0.7
								N	927			
								S	434			
1759+135	4C13.66	G?	-	2.3	-	21/10/86	0.25	Total	1281	1.2	742	0.5
								NW	26			
								N	143			
								S	1120			
1807+697	3C371	BL	0.051	5.8	3.9	22/05/86	0.25	Total	1401	0.30	1171	0.2
								Core	1220			
								Jet	88			
								SW	93			

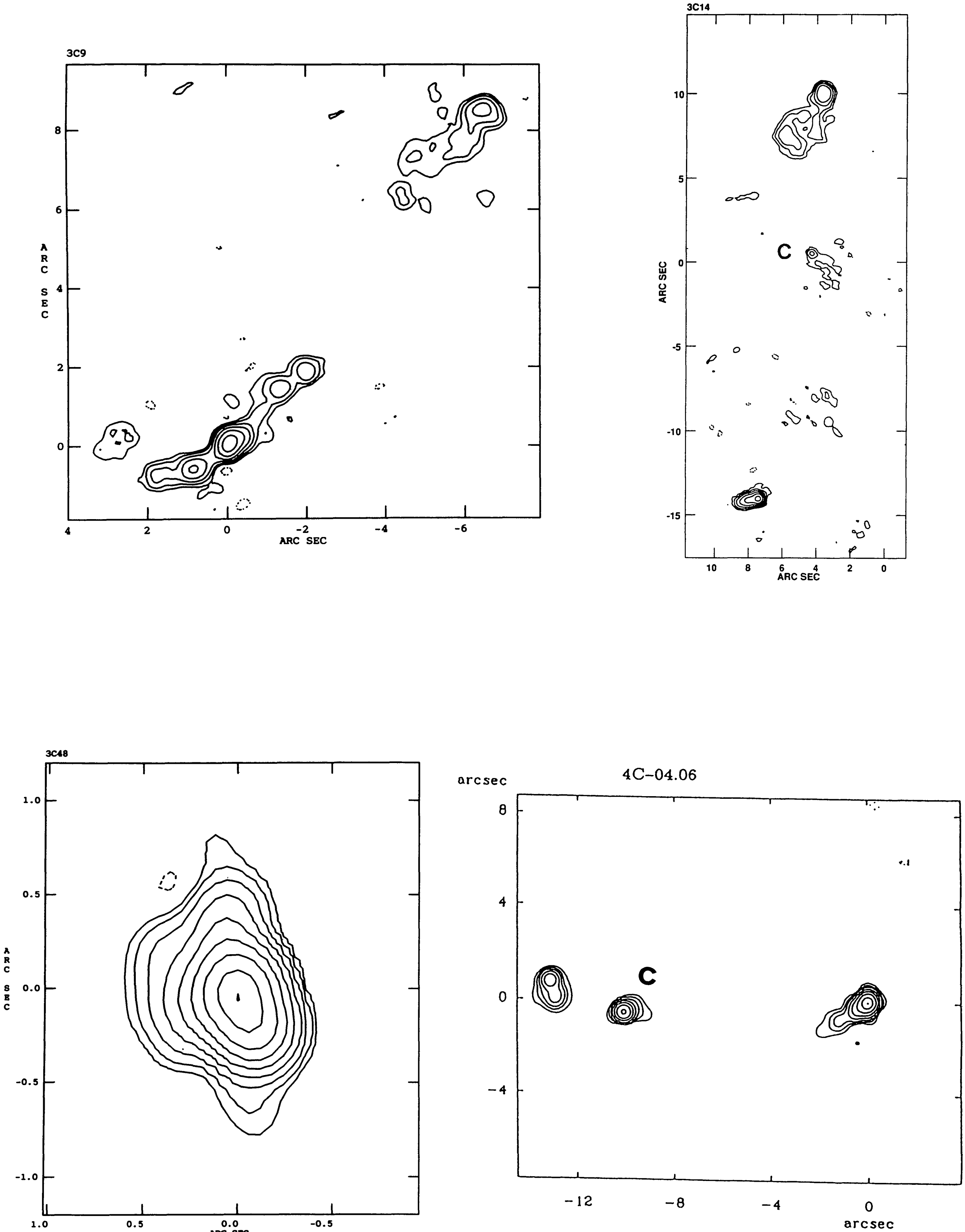

Fig. 1. Maps of the sources at 1.6 GHz. The restoring beams are given in Table 1 in each case. The contours are logrithmic, as percentages of peak flux density; the peak contour being 99 percent, others are 64, 32, 16, 8, 4, 2, 1, 0.5,.... Core components are marked with a 'C'

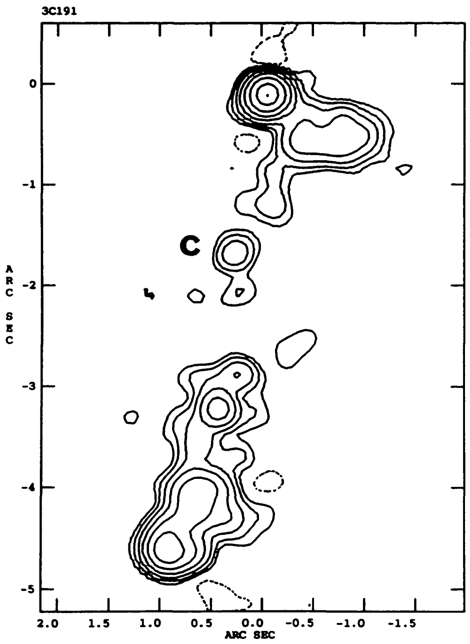

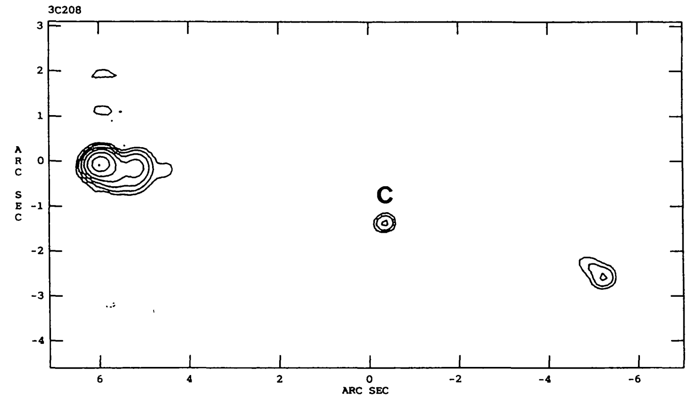

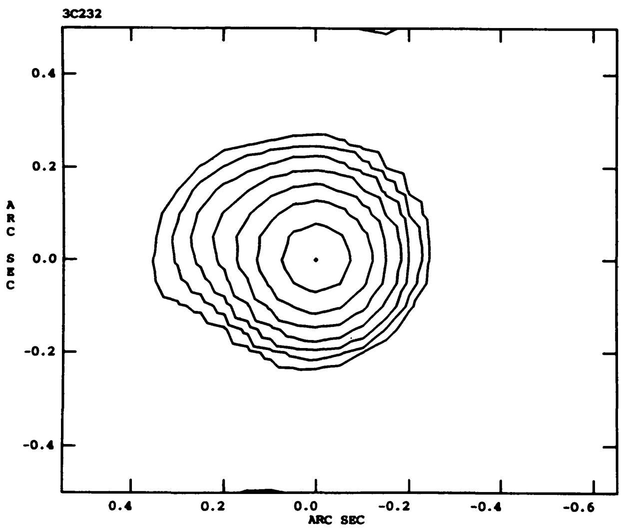

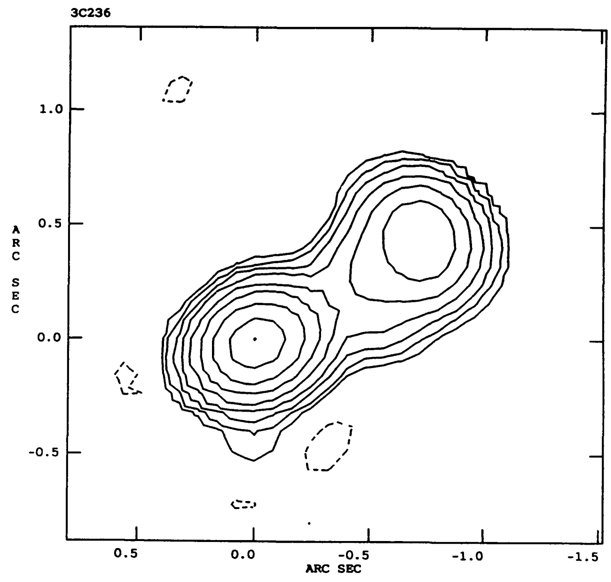

Fig. 1. continued

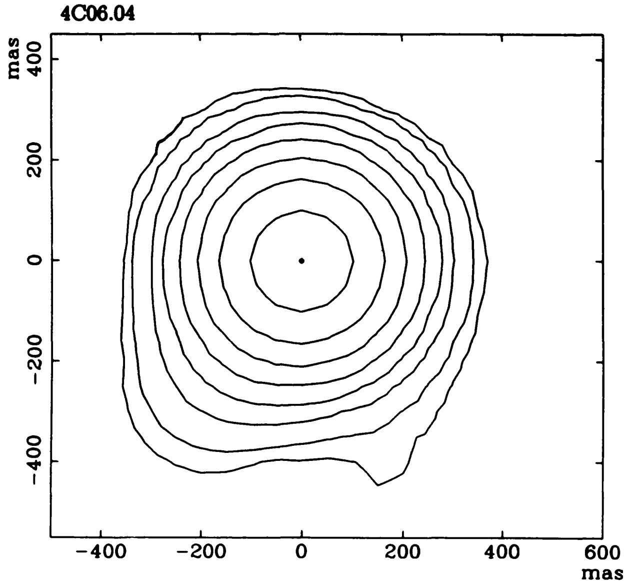

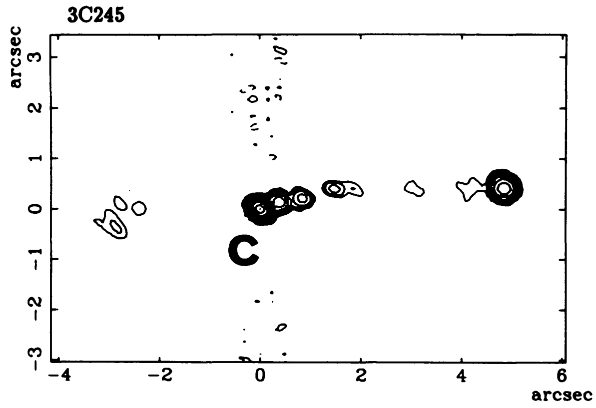

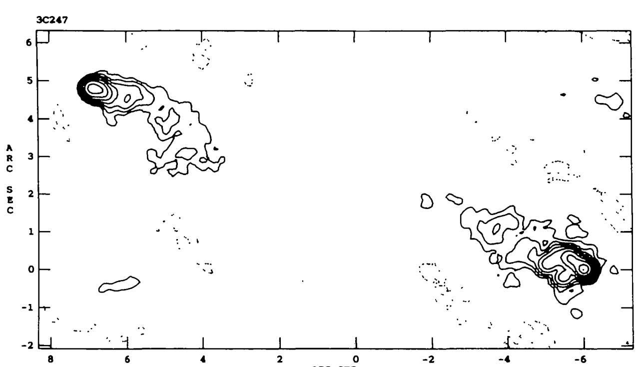

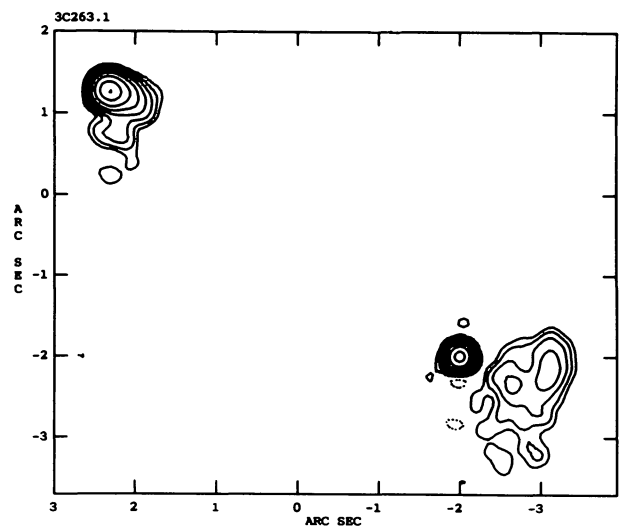

Fig. 1. continued

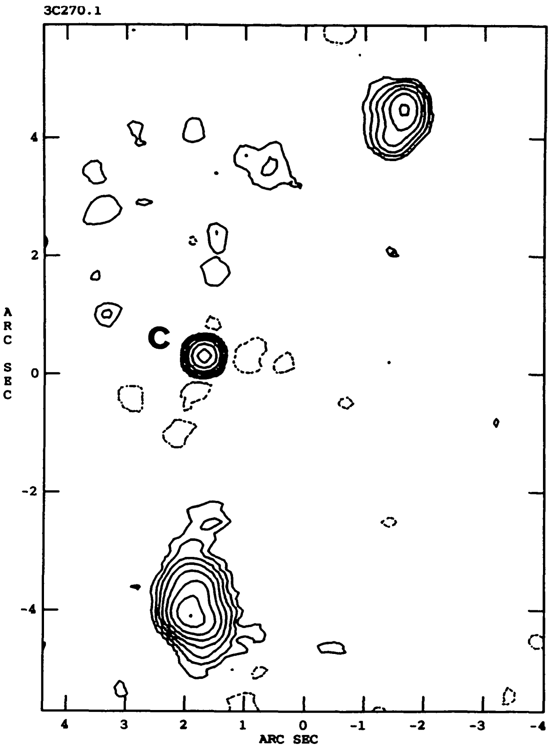

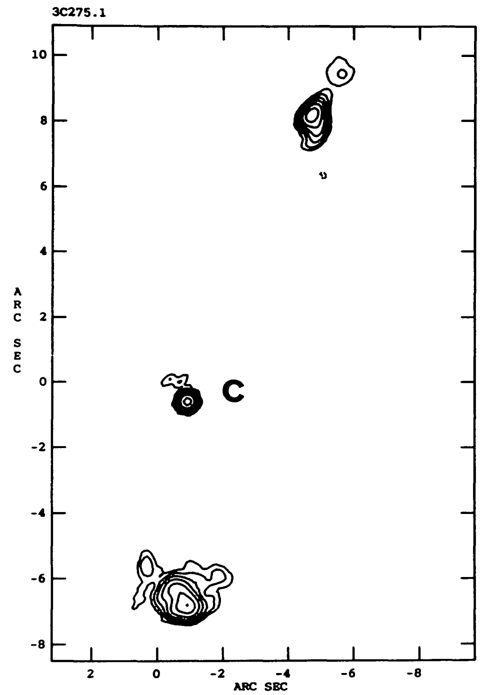

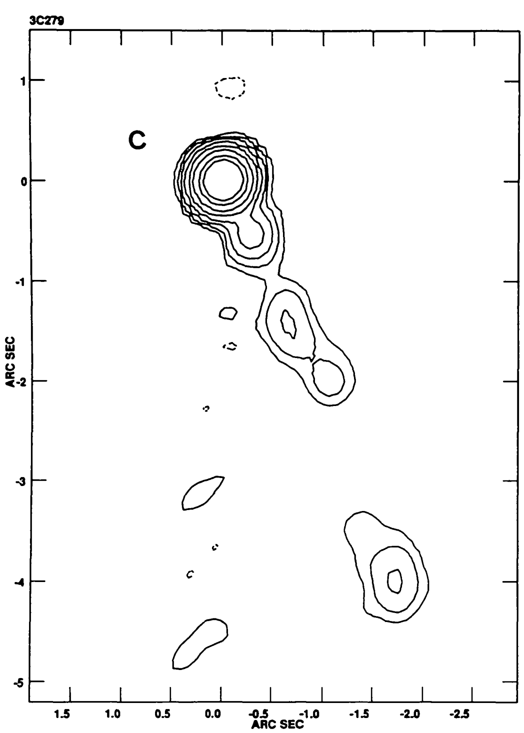

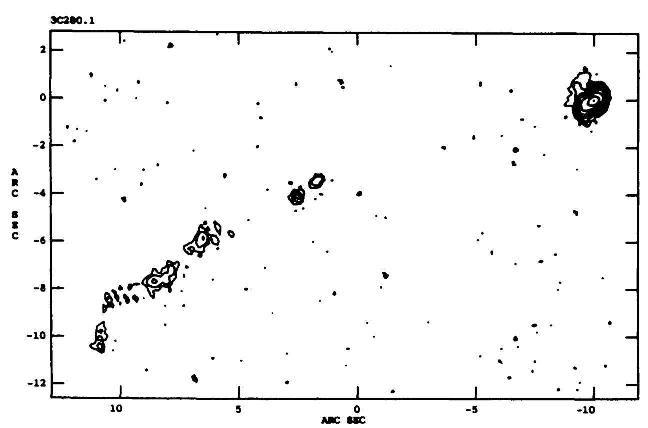

Fig. 1. continued

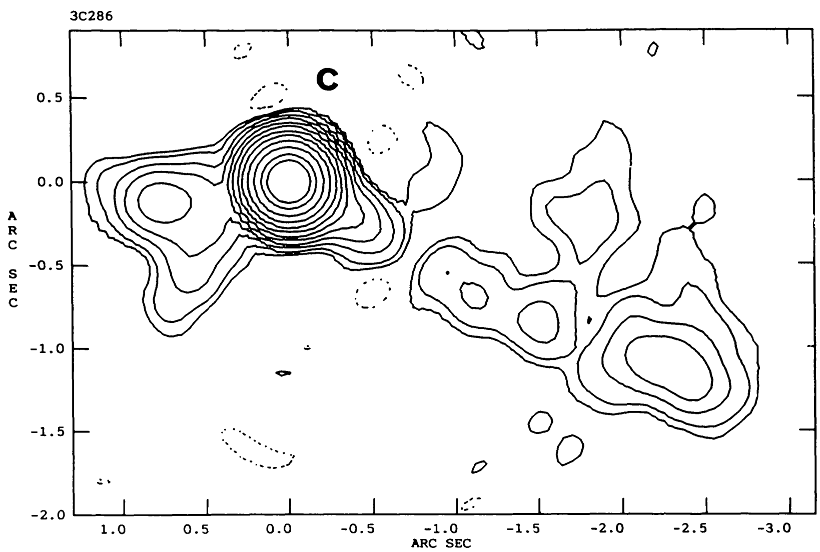

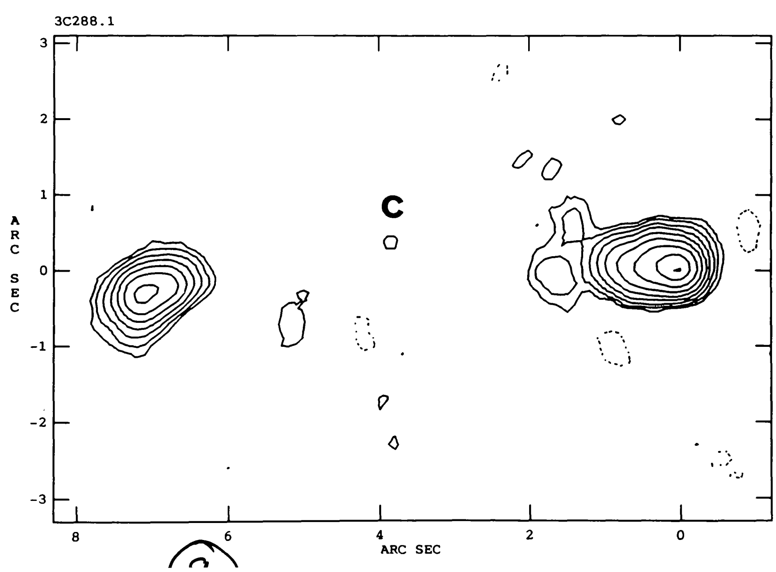

Fig. 1. continued

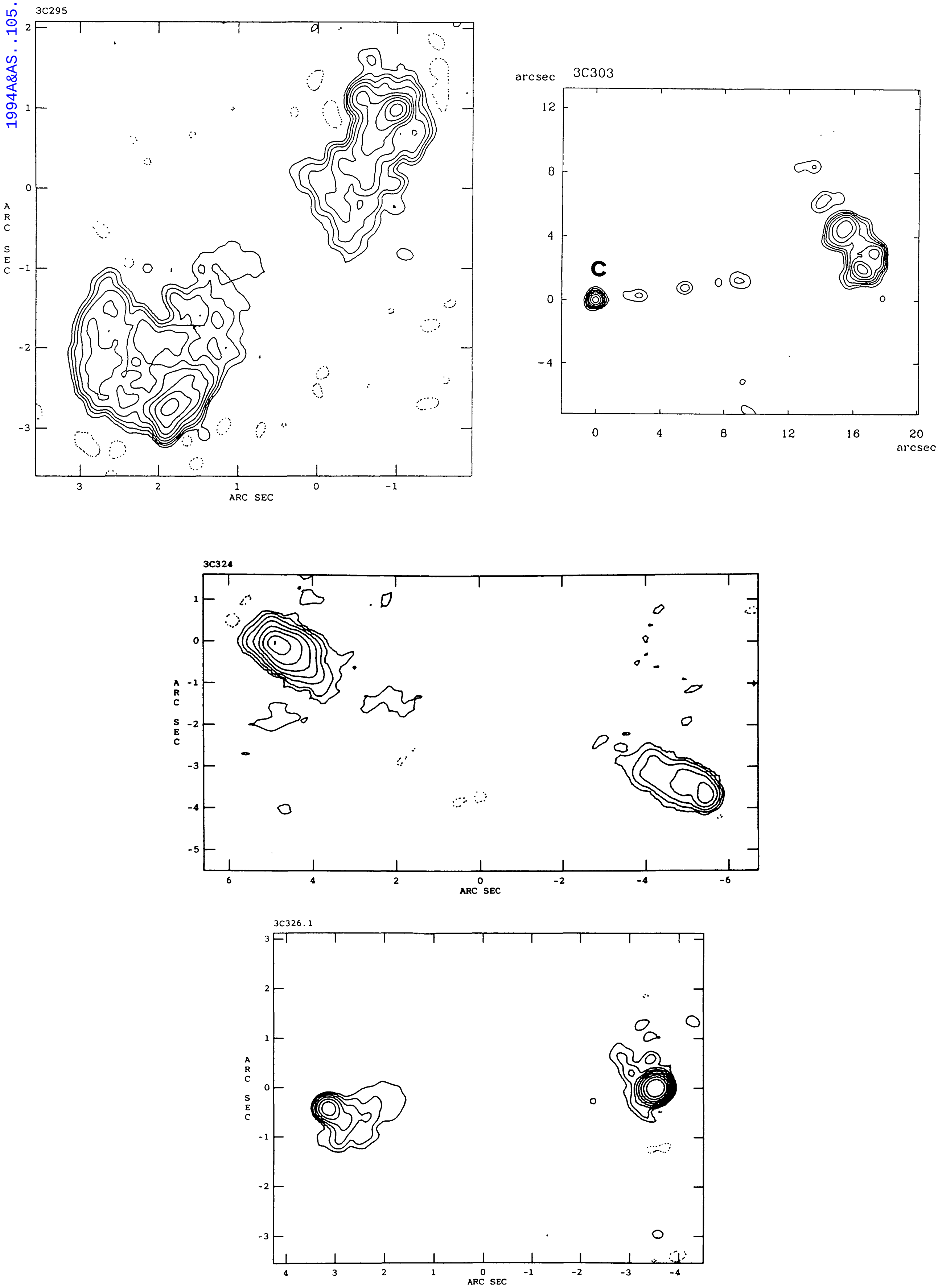

Fig. 1. continued

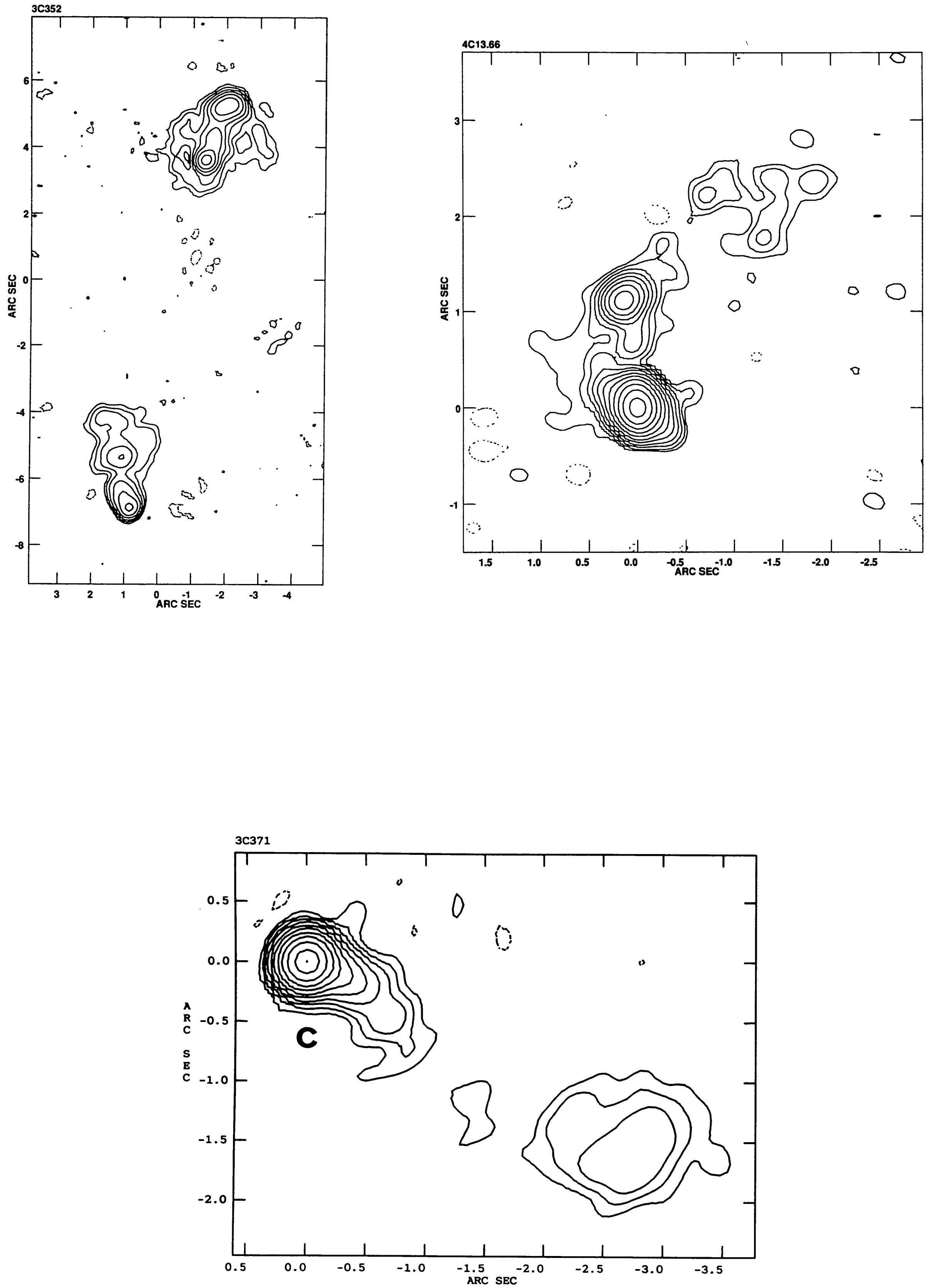

Fig. 1. continued